

Transport and Metabolic Pathway of Thymocartin (TP4) in Excised Bovine Nasal Mucosa

STEFFEN LANG*, PETER LANGGUTH, RAINER OSCHMANN†, BIRGIT TRAVING‡ AND HANS P. MERKLE

Department of Pharmacy, Swiss Federal Institute of Technology Zurich (ETH), Irchel Campus, Winterthurerstrasse 190, CH-8057 Zurich, Switzerland, and †Dr. Willmar Schwabe GmbH & Co., Willmar Schwabe Strasse 4, D-76227 Karlsruhe, Germany

Abstract

Thymocartin (TP4, Arg-Lys-Asp-Val) is the 32-35 fragment of the naturally occurring thymic factor (thymopoietin). Here studies on the nasal transport and metabolism of TP4 were performed. Freshly excised bovine nasal mucosa was taken as a model membrane. For permeation studies typical donor-receiver experiments (side-by-side) and finite-dose experiments with small volumes of highly concentrated solutions were carried out.

The metabolic pathway of TP4 in nasal mucosa was found to occur according to a typical aminopeptidase cleavage pattern, stepwise forming Lys-Asp-Val and Asp-Val. TP4 metabolism experiments under reflection kinetics showed a saturation profile above $0.5 \mu\text{mol mL}^{-1}$. A non-linear kinetic model consisting of three steps in sequence was sufficient to describe the kinetics: for the first step saturable Michaelis-Meet kinetics, and for the second and the third step first-order kinetics were assumed. The model was capable of simultaneously fitting the data for the full range of initial concentrations from 0.1 up to $1.0 \mu\text{mol mL}^{-1}$. Saturation kinetics was also found to be the prominent feature of the permeation experiments performed. In the lower concentration range ($< 0.4 \mu\text{mol mL}^{-1}$), transport of TP4 across nasal mucosa was controlled by metabolism, in the higher concentration range ($> 0.85 \mu\text{mol mL}^{-1}$) diffusion control became more important.

We conclude that enhancement of absorption can be achieved when nasal aminopeptidases are saturated, e.g. at high TP4 concentrations.

Thymopentin (TP5), the 32-36 fragment of the naturally occurring thymic factor, influences the immune system by promoting the differentiation of thymocytes and affecting the function of mature T-cells. Thymocartin (TP4) is the TP5 homologue that lacks the C-terminal Tyr. In preclinical studies the pharmacological effects of TP4 were comparable with those of TP5 (Kisfaludy et al 1985; Dènes et al 1987) indicating the therapeutic potential of TP4.

As an alternative to parenteral application, the patient-friendly delivery of TP4 by mucosal routes of entry is of major interest. The most common route of application for the systemic delivery of drugs, i.e. peroral dosing, is limited for most peptides due to extensive metabolism and poor mucosal permeability (Lee 1990). Hence various other application routes have been investigated for systemic peptide delivery. The nasal route is characterized by its leaky epithelium, lack of first-pass effect and good patient acceptance. In the past, the nose has been shown to be a suitable site of application for the systemic delivery of peptides, such as human calcitonin (Pontiroli et al 1989), insulin (Illum 1991), and desmopressin (Harris et al 1986). The nasal route may, therefore, be an interesting alternative for the systemic delivery of TP4.

The present study represents the first step in the evaluation of the feasibility of the nasal application for systemic delivery of TP4.

Materials and Methods

Chemicals

Thymocartin (TP4, Arg-Lys-Asp-Val), thymotrigan (TP3, Arg-Lys-Asp), Lys-Asp-Val, Arg-Lys, Asp-Val and Lys-Asp were kindly provided by Schwabe AG (Karlsruhe, Germany). Thymopentin (TP5, Arg-Lys-Asp-Val-Tyr) was purchased from Cilag AG (Schaffhausen, Switzerland). Arg, Lys, Asp, Val, sodium heptanesulfonic acid were from Fluka; Krebs Ringer buffer (KRB) from Sigma. The ion composition of KRB was (mM): $\text{MgCl}_2 \cdot 6\text{H}_2\text{O}$ 0.492; KCl 4.56; NaCl 119.8; Na_2HPO_4 0.70; NaH_2PO_4 1.5; NaHCO_3 15. The D-glucose content was 10 mM. All KRB solutions were saturated with prehumidified carbogen (95% O_2 / 5% CO_2) before use. All other chemicals were of analytical grade. For HPLC appropriate solvents of HPLC quality were used.

HPLC analyses

The HPLC system consisted of an autosampler AS2000, a gradient pump L-6200A, a UV-detector L-4250 and an integrator D-4270 (all from Merck AG, Basle, Switzerland). The compositions of the mobile phases A and B were: 0.5% (v/v) phosphoric acid containing 1 mM sodium heptanesulphonic acid for A, and a 1:1 (v/v) mixture of 0.5% (v/v) phosphoric acid containing 1 mM sodium heptanesulphonic acid and acetonitrile for B. A flow of 1 mL min^{-1} and a Lichrospher RP-18 column (Merck, Basle, Switzerland) of 25 cm length were applied. For the permeation studies a linear gradient from 100% to 55% A in 10 min was used, followed by 10 min at 55% A and a subsequent linear gradient from 55% to 0% A in 10 min. The UV detector was set at 214 nm. For the meta-

*Present address: S. Lang, Ciba-Geigy AG, Corporate Research Units, K-127.1.04 CH-4002 Basle, Switzerland.

Correspondence: H. P. Merkle, Department of Pharmacy, Swiss Federal Institute of Technology Zurich (ETH), Winterthurerstrasse 190, CH-8057 Zurich, Switzerland. Email: Hmerkle@pharma.ethz.ch

bolism studies the same mobile phases were used under the following conditions: a linear gradient from 100% to 75% A in 15 min, followed by 60% A from 15 to 35 min and a subsequent linear gradient from 60% to 0% A from 35 to 40 min. For TP5 analyses the method described by Hussain et al (1990) was applied. The mobile phase contained 0.1 M monobasic sodium phosphate : phosphoric acid : acetonitrile (916:5:60, v/v/v). A flow rate of 1 mL min⁻¹ and a LiChrospher 100 RP-18 column of 12.5 cm length (Merck AG, Basle, Switzerland) were used. Detection was by measuring UV absorbance at 214 nm.

Excised bovine nasal mucosa

Fresh bovine nasal mucosa was obtained at the local slaughterhouse in Zurich (Schlachthaus AG, Zurich, Switzerland). Tissue with nasal mucosa was excised from the noses of freshly slaughtered cattle (domestic brown, male and female). After removing the skin, tissue containing nasal mucosa was cut out with a sharp knife from the frontal part of the nasal conch (conchae nasales dorsales) above the *os incisivum* starting from the incisura nasoincisiva. The excised tissue was stored on ice during transport to the laboratory. At no more than 30 min after excision, the mucosa was separated from the underlying cartilage by blunt stripping using a pair of tweezers. Samples of 3–4 cm² were obtained and inserted into the diffusion chambers, the apical side of the tissue typically facing the donor compartment. For equilibration the mucosa was preincubated with KRB for 15–20 min.

Diffusion chambers

Commercially available side-by-side diffusion chambers (Side-Bi-Side, Crown Glass, Sommerville, NJ, USA) were used to perform nasal permeation and metabolism studies (Fig. 1). To ensure absence of chemical and physical instability of TP4, controls without excised mucosa were made. No relevant loss of TP4 was observed.

Metabolic pathway and metabolic rate

The metabolism of TP4 was studied using a reflection kinetics model. Briefly, only one chamber of the side-by-side diffusion set-up was used. The other chamber was replaced by an impermeable support block (Fig. 1, bottom). This principal set-up was adapted from that of Yu et al (1979). The nasal mucosa was prepared as described above and inserted into the half-cell, with the apical side facing the peptide solution. The diffusional flux of the peptide into the mucosa and the flux of the simultaneously formed metabolites were reflected at the impermeable support. Loss of substrate and formation of metabolites were monitored in the bulk solution. For equilibration the mucosa was incubated in pure KRB for 15–20 min. Then the bulk solution was replaced by 3 mL of a solution of TP4 in KRB. The peptide was studied in various concentrations ranging from 0.1 to 1 µmol mL⁻¹. At given time intervals of up to 90 min samples were taken from the bulk solution and analysed by HPLC. The identity of TP4 metabolites was determined by comparative HPLC analyses of potential metabolites for reference. In analogy to TP4, the metabolic degradation of Lys-Asp-Val was also investigated for comparison at a concentration of 0.3 µmol mL⁻¹. The absence of significant aminopeptidase leakage from the model membrane

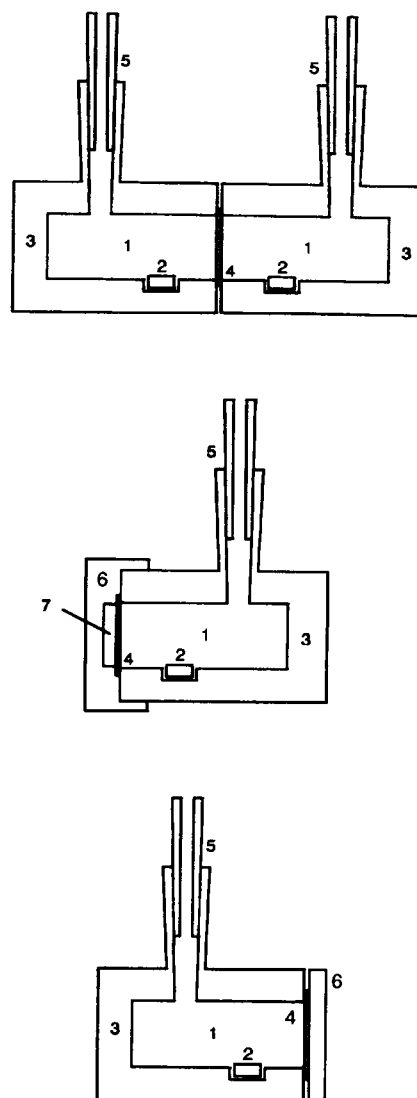


FIG. 1. Top. Schematic cross section of two-chamber side-by-side diffusion set-up used for permeation studies. Middle. One-chamber set-up with a porous matrix support for finite dose permeation studies. Bottom. One-chamber set-up for metabolism studies under reflection kinetics. (1) donor- and receiver compartment, volume each 3 mL, (2) magnetic stirrer 600 rev min⁻¹, (3) thermal jacket 37°C, (4) excised bovine nasal mucosa, (5) stoppers for controlled gas flow, carbogen (95% O₂/5% CO₂), (6) holder for membrane (7) porous matrix support.

was verified by further incubation of peptide solutions which were previously in contact with the mucosa.

The metabolic rates, v_M , of TP4 were calculated from the linear segments of the concentration-time profiles, $(d[TP4]/dt)_{SS}$, in the steady state (5–60 min) according to equation 1, with A [cm²] = surface area of the model membrane, and V [mL] = volume of the bulk solution:

$$v_M = - \left(\frac{d[TP4]}{dt} \right)_{SS} \frac{V}{A} \quad (1)$$

Kinetic analysis of TP4 metabolism

The kinetic modelling of the metabolic cleavage of TP4 (Arg-Lys-Asp-Val) and of its metabolites Lys-Asp-Val and Asp-Val



FIG. 2. Kinetic model for the nasal mucosal metabolism of thymocartin (TP4; Arg-Lys-Asp-Val).

in the nasal mucosa was based on kinetic analysis according to the catenary model given in Fig. 2. Metabolism of TP4 was assumed to follow saturable Michaelis-Menten-type kinetics. The two subsequent steps were represented by two first-order kinetics steps in sequence, resulting in a set of non-linear and first-order differential equations.

$$-\frac{d[TP4]}{dt} = \frac{v_{\max}[TP4]}{K_m + [TP4]} \quad (2)$$

$$\frac{d[Lys - Asp - Val]}{dt} = \frac{v_{\max}[TP4]}{K_m + [TP4]} - k_{tr}[Lys - Asp - Val] \quad (3)$$

$$\frac{d[Asp - Val]}{dt} = k_{tr}[Lys - Asp - Val] - k_{di}[Asp - Val] \quad (4)$$

The numerical solution of this set of differential equations was by means of TOPFIT (Version 2.02, Gustav Fischer Verlag, Stuttgart, Germany). For regression analysis four different data sets of the means ($n = 4$) of concentrations of TP4, Lys-Asp-Val and Asp-Val versus time were used (0.1, 0.2, 0.5 and 1 $\mu\text{mol mL}^{-1}$). A simultaneous fit of the means of all four data sets was made. To relate the concentrations calculated to the actually measured concentrations, in each equation an apparent distribution volume was included as model parameter to be optimized. This was implemented in the model as a dimensionless scaling factor, $V_{\text{app}}/V_{\text{act}}$, where V_{app} is the apparent and V_{act} the actual volume (3 mL) of the receiver compartment. Physically the scaling factor serves to account for potential binding of the substrate and/or the metabolites to the mucosa. The parameters to be fitted were K_m , V_{\max} , k_{tr} , k_{di} and the apparent distribution volumes $V_{\text{app},1}$, $V_{\text{app},2}$ and $V_{\text{app},3}$ of TP4 and of its metabolites Lys-Asp-Val and Asp-Val, respectively.

Permeation kinetics

For the permeation studies the KRB used for equilibration was replaced by the peptide solution on the donor side and by pure

KRB on the receiver side (Fig. 1, top). The initial TP4 concentrations ranged from 0.06 to 0.85 $\mu\text{mol mL}^{-1}$. At given time intervals up to 55 min, samples were taken from both compartments and analysed. The sample volume was replaced by pure KRB. Permeation data was corrected for the dilution of the receiver solution. For the donor compartment dilution was neglected. The viability of the model membrane was monitored by electrophysiological parameters. Steady-state values of the potential difference (P.D.) and the short-circuit current (I_{sc}) were reasonably constant and in a typical range: P.D. = 0.9–2.9 mV (sub-mucosa positive), $I_{\text{sc}} = 36\text{--}66 \mu\text{A cm}^{-2}$. Data from membranes outside the limits were discarded.

Effective permeability coefficients P_{eff} [cm s^{-1}] were calculated according to equation 5:

$$P_{\text{eff}} = \left(\frac{d[TP4]}{dt} \right)_{\text{ss}} \frac{V}{AC_D} \quad (5)$$

where $(d[TP4]/dt)_{\text{ss}}$ = change of concentration in time [s] during steady-state, A [cm^2] = permeation area, V [mL] = volume of the receiver compartment and C_D [mol mL^{-1}] = initial concentration in the donor compartment.

Permeation experiments with TP5 were performed in the same way.

Finite dose permeation of TP4

The experimental set-up (Fig. 1, middle) used for the finite dose permeation studies was as follows: a porous gelatine matrix disk (diameter 10 mm, thickness 0.5 mm; Spongostan, Novo Nordisk Inc., Zurich, Switzerland) was soaked with 50 μL of a TP4 solution containing 1000 μg (approx. 40 $\mu\text{mol mL}^{-1}$). The disk loaded with peptide was then brought in contact with the apical side of the model membrane. Up to 45 min, samples were taken from the receiver solution and analysed by HPLC.

Results and Discussion

Metabolism studies

A typical HPLC chromatogram of a sample solution of TP4 after contact with excised bovine nasal mucosa showed the main peak of TP4 and several additional peaks of metabolites that are neither present in pure KRB solutions incubated with the mucosa, nor in TP4 solutions treated under similar conditions but without contact with the mucosa (data not shown). To

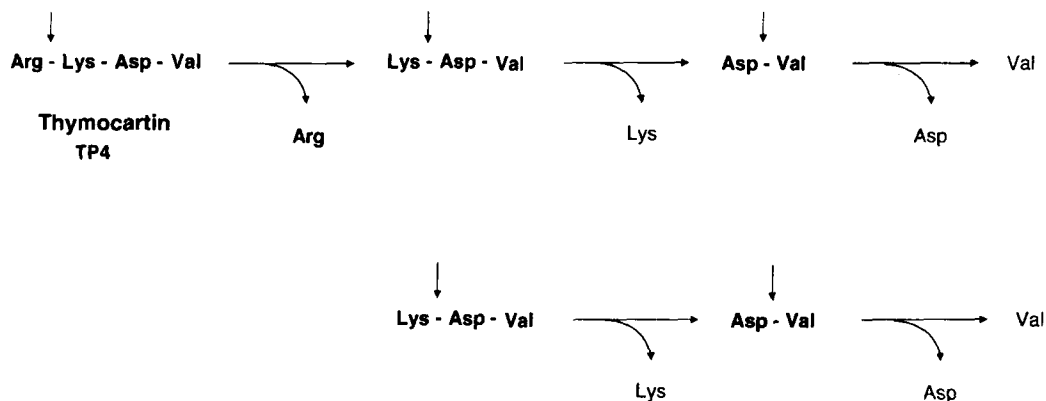


FIG. 3. Metabolic pathways of thymocartin (TP4) and of its metabolite Lys-Asp-Val in excised bovine nasal mucosa. Arrows indicate cleavage positions by mucosal aminopeptidases. The metabolites directly detected by HPLC in addition to TP4 are given in bold.

Table 1. Typical nasal metabolism of TP4. Molar percentages of TP4, of its metabolites Lys-Asp-Val and Asp-Val, and total recovery after 60 min during in-vitro metabolism studies (reflection kinetics) with excised bovine nasal mucosa.

Peptide	Initial peptide concentration (mmol mL ⁻¹)	TP4 ^a (%)	Lys-Asp-Val ^a (%)	Asp-Val ^a (%)	Total recovery ^a (%)
TP4	0.1	31.9 ± 4.9	12.8 ± 1.7	n.d. ^b	44.7 ± 6.6
	0.2	56.6 ± 4.4	21.6 ± 2.3	17.1 ± 3.3	95.3 ± 10.0
	0.5	67.8 ± 5.7	10.7 ± 0.5	10.6 ± 2.9	89.1 ± 9.1
Lys-Asp-Val	1.0	73.9 ± 2.3 ^c	6.1 ± 1.2	7.6 ± 1.5	87.6 ± 5.0
	0.3		29.6 ± 6.4	32.9 ± 5.5	62.5 ± 11.9

^aMeans ± s.d., n = 4. ^bNot detectable. ^cNo data available.

identify the TP4 metabolites all potential peptide fragments and amino acids which may have been formed by enzymatic cleavage of the TP4 peptide linkages (Arg-Lys-Asp, Lys-Asp-Val, Arg-Lys, Lys-Asp, Asp-Val, Arg, Lys, Asp, Val) were analysed by HPLC under the same conditions. The verification of the identity of the metabolites was achieved by adding reference standards to the TP4 incubation solutions before HPLC analyses. Arg-Lys-Asp (TP3) was not found as a metabolite of nasal TP4 degradation.

Metabolic pathway of TP4

The metabolic pathway of TP4 derived from the HPLC analyses is summarized in Fig. 3. In analogy with TP4, the same pattern was also observed for Lys-Asp-Val when incubated under the same conditions. The amino acids Asp, Val, and Lys indicated in Fig. 3 were not detectable under the conditions of the analysis and in the concentration range studied ($\leq 0.05 \mu\text{mol mL}^{-1}$). HPLC analysis of TP4 degradation alone could not exclude the theoretical formation of Lys-Asp in the course of the metabolic pathway, potentially by C-terminal cleavage of Lys-Asp-Val, due to an overlay of the peaks of Lys-Asp and Arg under the HPLC conditions applied. However, corresponding studies on the metabolism of Lys-Asp-Val (as a control) showed clearly that in the nasal mucosa Lys-Asp-Val is not subject to significant C-terminal cleavage (Fig. 3). Therefore, it was concluded that the absence of C-terminal cleavage is also typical for the metabolic pathway of TP4.

The stepwise cleavage of single amino acids from the N-terminus is specific for aminopeptidases. The presence of aminopeptidase activity in the nasal mucosa is well established in various species, and in human mucosa (Peter et al 1992).

Metabolism kinetics of TP4

TP4 was extensively degraded in the whole concentration range studied, with lower relative degradation rates at the higher concentrations. To compare the degradation kinetics for each concentration studied the metabolic rates (v_m) were estimated from the approximately linear parts of the concentration-time profiles (equation 1). The reaction followed non-linear kinetics; the metabolic rates are typically concentration dependent and form a plateau in the high concentration range (Fig. 5). This is indicative of a saturation of the metabolizing enzymes as TP4 concentrations increase.

At the lowest TP4 concentrations studied ($0.1 \mu\text{mol mL}^{-1}$) and for the studies with Lys-Asp-Val the total molar recovery was about 40–60% (Table 1), whereas at the higher TP4

concentrations studied the total recoveries averaged 90%. The remainder is attributed to undetectable amino acids formed by aminopeptidase cleavage of Asp-Val; because of the non-linear kinetics, this is more important at the lower initial TP4 concentrations.

Kinetic analysis of TP4 metabolism

The empirical kinetic model applied to simultaneously analyse the kinetics of TP4 metabolism and of its metabolites Lys-Asp-Val and Asp-Val is shown in Fig. 2. Both the experimental data and the corresponding numerically fitted concentration vs time profiles are included in Fig. 4. The simultaneous non-linear fit covering the means of all four data sets resulted in a reasonably close approximation of the experimental data ($r = 0.95$). When using the individual data sets ($n = 4$) instead of the means, the regression analysis was unstable. The non-linear kinetic model applied appears to be well-suited for the full range of the data sets available (initial TP4 concentrations from 0.1 to $1.0 \mu\text{mol mL}^{-1}$). Thus, saturation kinetics of TP4 cleavage is the most satisfactory model for the kinetics, and is consistent with the information given in Fig. 5.

The parameter estimates for the fit of the model are given in Table 2. The apparent volumes of distribution were 2.9 mL for TP4 and 2.5 mL for Asp-Val were in reasonable agreement with the volume of the bulk solution of 3 mL in the experimental design. For Lys-Asp-Val the apparent volume of distribution was 8.75 mL. The increase in the apparent volume may indicate binding of the tripeptide to the mucosa, thus increasing its apparent volume of distribution. Due to the very low concentrations of the metabolic intermediate Lys-Asp-Val, some binding to the mucosa may have a dramatic influence on the concentrations found in the bulk solution. This is in sharp contrast to TP4 with its high concentrations in the bulk medium, which are unlikely to be significantly affected by (relatively) minor binding to the mucosa.

Permeation kinetics

The concentration-time profiles of TP4 and Lys-Asp-Val in both the donor and the receiver compartment are shown in Fig. 6 (left) for an initial donor concentration of $0.85 \mu\text{mol mL}^{-1}$ TP4. Less than 1% of the donor content of TP4 was found in the receiver compartment after 55 min. The concentrations of Lys-Asp-Val in the receiver compartment were about three-fold higher than those of TP4.

The permeation of TP4 was also studied at two lower initial concentrations ($0.06 \mu\text{mol mL}^{-1}$ and $0.4 \mu\text{mol mL}^{-1}$). For all three concentrations the effective permeability coefficients

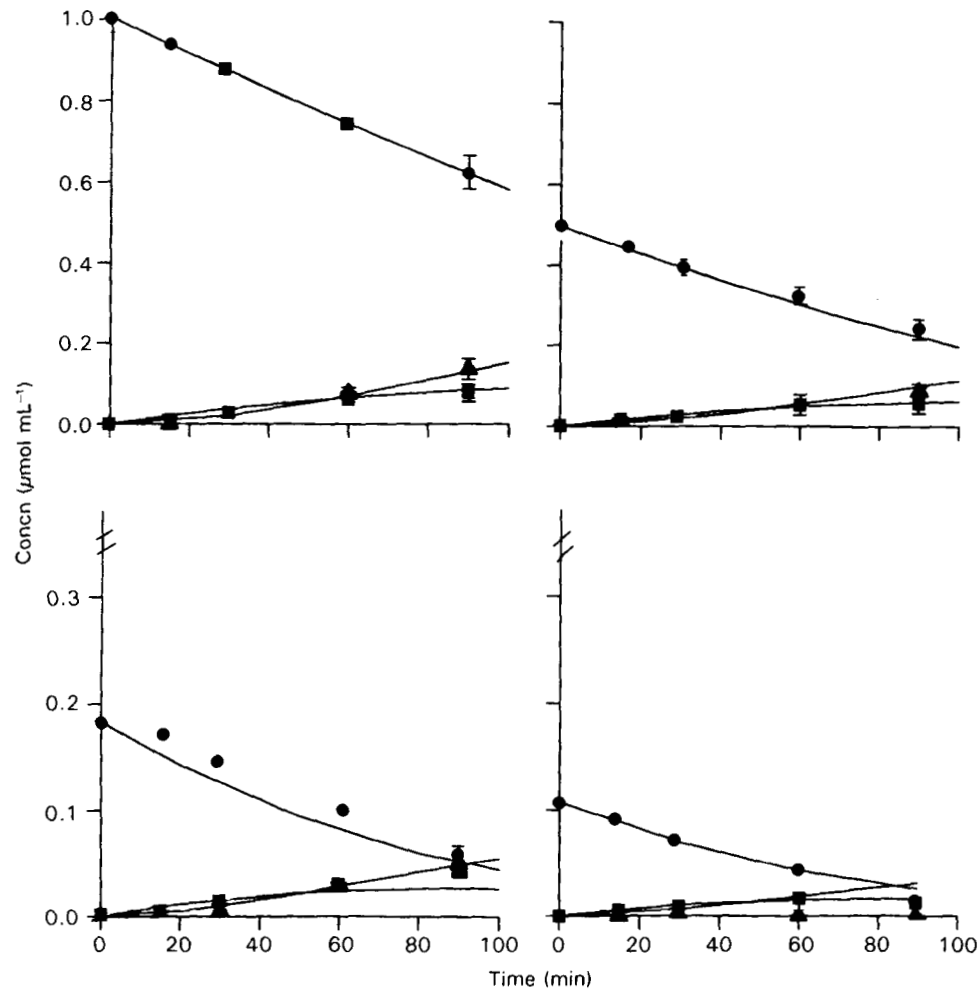


FIG. 4. Metabolic degradation of TP4 in excised nasal mucosa. Concentration-time profiles of TP4 (●), and of its metabolites Lys-Asp-Val (■), and Asp-Val (▲). The initial TP4 concentrations applied were from 0.1 to 1.0 $\mu\text{mol mL}^{-1}$ as indicated on the ordinates of the four graphs (reflection kinetics; means \pm s.d., $n = 4$, s.d. partly within symbols). The lines represent simultaneous fits for all four data sets, based on non-linear kinetic analysis as presented in Fig. 2 and equations 2-4. The graph indicates reasonable agreement between the experimental data and the simultaneous fits.

(P_{eff}) were calculated from the concentration-time profiles in the receiver compartment under steady-state conditions (equation 2). For the lowest TP4 concentration studied (0.06 $\mu\text{mol mL}^{-1}$), the P_{eff} value was calculated on the basis

of the cumulative amount permeated at 55 min only, because TP4 was below the detection limit up to 45 min of permeation. The P_{eff} values calculated increased with increasing concentrations (Fig. 7). On increasing the donor concentration from 0.4 to 0.85 $\mu\text{mol mL}^{-1}$, P_{eff} increased 8-fold.

At 4°C, the permeation of 0.85 $\mu\text{mol mL}^{-1}$ TP4 was lower and the metabolic degradation was negligible (Fig. 6). The

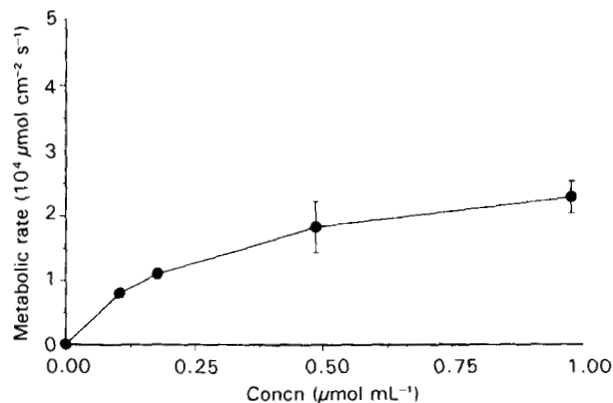


FIG. 5. Non-linear kinetics of TP4 metabolism in excised bovine nasal mucosa (reflection kinetics; means \pm s.d., $n = 4$, s.d. partly within symbols).

Table 2. Parameter estimates based on simultaneous non-linear kinetics analysis as presented in Fig. 2 and equations 2-4 for the nasal metabolic degradation of TP4 and its metabolites Lys-Asp-Val and Asp-Val.

Parameter	Estimate
$V_{\text{app},1}^a$	2.9 mL
$V_{\text{app},2}^a$	8.8 mL
$V_{\text{app},3}^a$	2.5 mL
v_{max}	0.0174 $\text{mmol mL}^{-1} \text{cm}^{-2} \text{min}^{-1}$
K_m	0.931 mmol mL^{-1}
k_{tri}	0.0101 min^{-1}
k_{di}	0.0056 min^{-1}

^a $V_{\text{app},1}$, $V_{\text{app},2}$ and $V_{\text{app},3}$ represent the apparent distribution volumes of TP4, Lys-Asp-Val and Asp-Val, respectively.

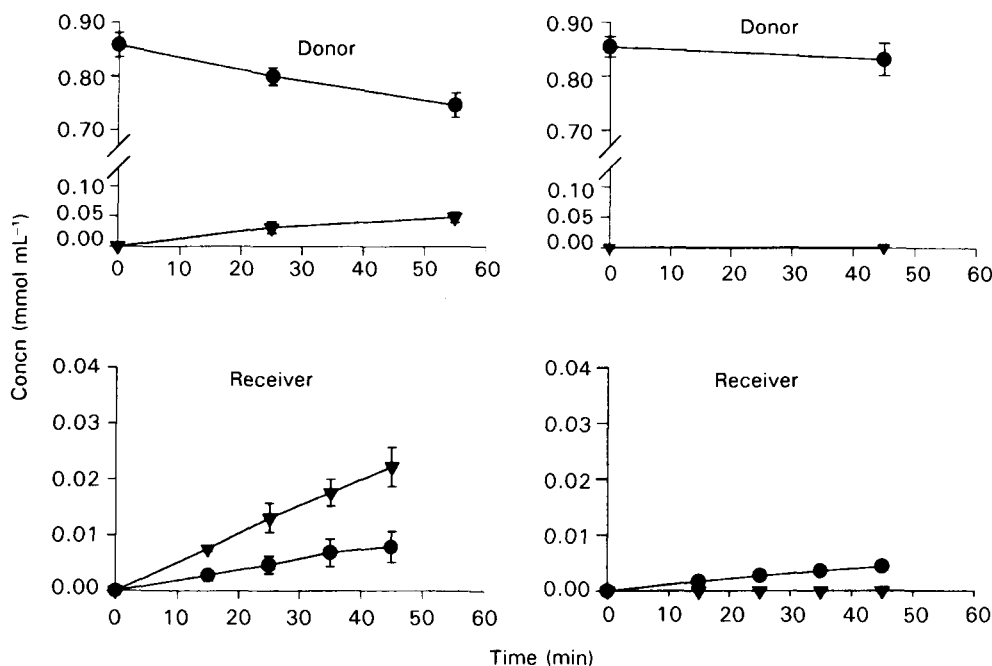


FIG. 6. In-vitro transport of TP4 across excised bovine nasal mucosa at 37°C (left) and at 4°C (right). Concentration vs time profiles of TP4 (●) and its metabolite Lys-Asp-Val (▼) in the donor (upper panels) and receiver compartments (lower panels). Initial TP4 concentration was 0.85 $\mu\text{mol mL}^{-1}$. Means \pm s.d., n = 4-6, s.d. partly within symbols.

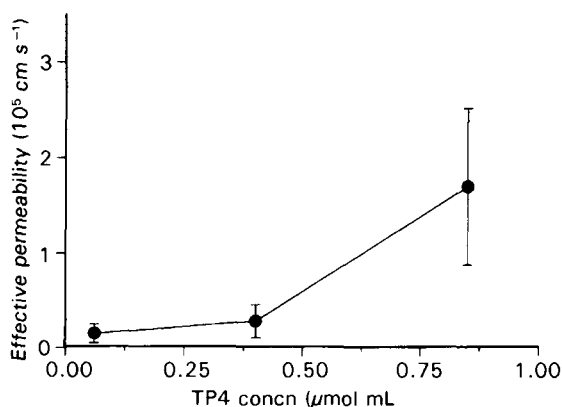


FIG. 7. Effective permeability coefficients (P_{eff}) of TP4 across excised bovine nasal mucosa (means \pm s.d., n = 4-6).

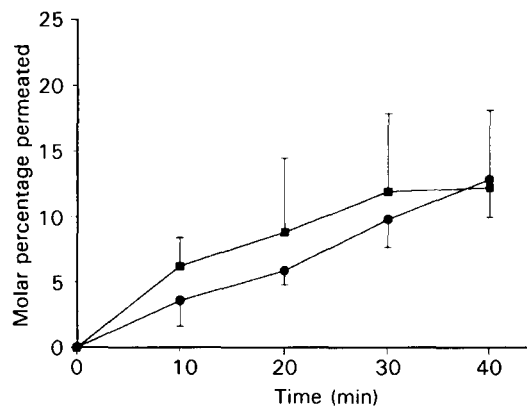


FIG. 8. Finite-dose permeation of TP4 across excised bovine nasal mucosa. The matrix support was loaded with 1000 μg of TP4 in 50 μL . TP4 (■), Lys-Asp-Val (●). Means \pm s.d., n = 4.

relatively temperature-insensitive permeation rate of TP4 was indicative of a diffusion-controlled passive transfer of TP4 across the nasal mucosa, and excludes active transport.

The permeation of TP4 is strongly influenced by a concentration-dependent mechanism (Fig. 7). Based on the data obtained by reflection kinetics (Figs 4 and 5), the metabolic degradation is concluded to be of prime importance for the concentration-dependent TP4 permeation. This is supported by the fact that the P_{eff} value obtained at the highest concentration studied (0.85 $\mu\text{mol mL}^{-1}$) was found to be minimally influenced by the metabolic degradation, as indicated by the low differences between corresponding permeation studies at 37 and 4°C. Thus, in the high concentration range the metabo-

lizing enzymes appear to be saturated. Hence, the P_{eff} value of $1.70 \times 10^{-5} \text{ cm s}^{-1}$ at 0.85 $\mu\text{mol mL}^{-1}$ is assumed to represent the intrinsic permeability of TP4.

At lower initial TP4 concentrations the metabolic degradation is assumed to function as a major barrier against nasal transfer. At this concentration range the kinetics of metabolism were found to be non-saturated. This would explain the lower permeation rates and lower P_{eff} values compared with the values at higher concentration.

Because of the small molecular size and the high hydrophilicity of TP4, its diffusional transfer across the nasal mucosa may be assumed to occur via the paracellular tight-junctional pathway. In contrast, the permeation pathway and

the transfer mechanism of the primary TP4 metabolite, Lys-Asp-Val, across the nasal mucosa is less understood. For interpretation of the permeation profile of Lys-Asp-Val (Fig. 6) it is interesting to see that its rate of appearance in the donor (55 min: $0.048 \mu\text{mol mL}^{-1}$) was about twice that in the receiver (45 min: $0.022 \mu\text{mol mL}^{-1}$). More detailed knowledge on the distribution and location of the aminopeptidase activity in the nasal mucosa may help to understand this observation.

Comparison of TP4 and TP5

Corresponding studies on nasal permeation were also performed with thymopentin (TP5). TP5 is a homologue of TP4 and carries an additional C-terminal Tyr. By analogy with TP4, TP5 was readily metabolized in the nasal mucosa as evaluated by HPLC of a TP5 receiver solution after 30 min of permeation (HPLC data not shown). The rate of TP5 metabolism in the donor compartment was in the same range as observed for TP4, i.e. 14% TP4 vs 11% TP5 were metabolized within 45 min of permeation at an initial donor concentration of approx. $0.85 \mu\text{mol mL}^{-1}$. Comparative HPLC analyses with TP4 (Arg-Lys-Asp-Val) and TP3 (Arg-Lys-Asp) led to the conclusion that the two TP-homologues do not represent nasal metabolites of TP5 (HPLC data not shown).

The permeability coefficients of TP4 and TP5 at $0.85 \mu\text{mol mL}^{-1}$ initial donor concentration were found to be in the same range: 1.70 ± 0.83 vs 0.92 ± 0.34 ($10^{-5} \text{ cm s}^{-1}$ respectively (means \pm s.d., $n = 4$)).

Finite dose permeation of TP4

Both the native TP4 and its primary metabolite, Lys-Asp-Val, were found to permeate at approximately the same rate (Fig. 8). Preliminary studies at a lower dose ($500 \mu\text{g}$) showed much lower relative permeation rates for the native peptide (about 2% after 40 min; data not shown), whereas the relative concentrations of Lys-Asp-Val in the receiver compartment were increased fourfold. The observation of enhanced permeability at higher concentrations is in good agreement with the results

of the side-by-side permeation studies. Administration of small volumes of highly concentrated solutions may result in more efficient delivery across the mucosal epithelium. In light of the dramatic absorption enhancement observed with therapeutic peptides when administered in the form of peptide-loaded particles (Critchley et al 1994), we suggest that absorption enhancement by concentration-dependent local saturation of the metabolic capacity may become another factor.

References

- Critchley, H., Davis, S. S., Farraj, N. F., Illum, L. (1994) Nasal absorption of desmopressin in rats and sheep. Effect of bioadhesive microsphere delivery system. *J. Pharm. Pharmacol.* 46: 651–656
- Dènes, L., Szende, B., Hajos, G., Szporny, L., Lapis, K. (1987) Therapeutic possibilities of thymopentin fragments (TP3 and TP4) based on experimental animal models. *Drugs Expl. Clin. Res.* XIII: 279–287
- Harris, A. S., Nilsson, I. M., Wagner, Z. G., Alkner, U. (1986) Intranasal administration of peptides: nasal deposition, biological response, and absorption of desmopressin. *J. Pharm. Sci.* 75: 1085–1088
- Hussain, M. A., Koval, C. A., Shenvi, A. B., Aungst, B. J. (1990) An aminoboronic acid derivative inhibits thymopentin metabolism by mucosal membrane aminopeptidases. *Life Sci.* 47: 227–231
- Illum, L. (1991) Nasal delivery of peptides, factors affecting nasal absorption. In: Crommelin, D. J. A., Midha, K. K. (eds), *Topics in Pharmaceutical Sciences*, Medpharm, Stuttgart, pp 71–82
- Kisfaludy, L., Neyki, O., Schön, I., Dènes, L. (1985) European Patent No. 0067425 B1
- Lee, V. H. L. (1990) Protease inhibitors and penetration enhancers as approaches to modify peptide absorption. *J. Contr. Rel.* 13: 213–223
- Peter, H., Wunderli-Allenspach, H., Gammert, C., Merkle, H. P. (1992) Human nasal cell culture to study biotransformation of peptides. *Eur. J. Pharm. Biopharm.* 38: S31
- Pontiroli, A. E., Alberetto, M., Calderara, A., Pajetta, E., Yu, C. D., Fox, J. L., Ho, N. F. H., Higuchi, W. I. (1979) Physical model evaluation of topical prodrug delivery—simultaneous transport and bioconversion of vidarabin-5-valerate II: Parameter determinations. *J. Pharm. Sci.* 68: 1347–1357
- Yu, C. D., Fox, J. L., Ho, N. F. H., Higuchi, W. I. (1979) Physical model evaluation of topical prodrug delivery—simultaneous transport and bioconversion of violarabin-5-valerate II: parameter determinations. *J. Pharm. Sci.* 68: 1347–1357